

Research on the uprising dynamics of a double-carriage overhead crane system

X Yao*, X Guo, Y Feng, and C Yu

Xi'an Research Institute of Hi-Tech, Hong-qing Town, Xi'an, People's Republic of China

The manuscript was received on 28 November 2009 and was accepted after revision for publication on 9 April 2010.

DOI: 10.1177/09544062JMES2131

Abstract: The dynamic characteristics, in the uprising phase, of an overhead crane carrying two carriages and a cylindrical payload are studied in this article. The crane system investigated mainly consists of a twin beam, two carriages, a rigid payload, and two wire ropes. A new analytical model, in which the beam, carriages, payload, and wire ropes are, respectively, considered as uniform Euler–Bernoulli beam, lumped masses, rigid body, and springs, is presented to describe the uprising dynamics of the specific crane system. The most distinguished characteristic of the model is the dynamic coupling deriving from the presence of a flexible beam, carriages, and the cylindrical payload.

The kinetic and potential energies, during the pre-tensing and lifting phases, of the components in the system are presented in particular. Then, utilizing the Rayleigh–Ritz method, one can obtain the differential equations of the dynamic system substituting the energy into Lagrange's equation. The differential equations are numerically solved by the fourth-order Runge–Kutta method, and then some useful results representing the dynamic features of the system are obtained according to the calculation. The validity of the analytical model is demonstrated by an equivalent FE model created by ANSYS and ADAMS. Comparison of the results, obtained by two distinct approaches, indicates good agreements, which can be the validity evidence of the analytical model.

Keywords: overhead crane, dynamic model, mass-loaded beam, uprising dynamics, system simulation

1 INTRODUCTION

The primary use of an overhead crane is in the transfer of payloads from one location to another. In the trans-shipment of cylindrical equipment, henceforth called payload, the equipment needs to be horizontally upraised and fleetly trans-shipped to the prearranged location utilizing a double-carriage overhead crane. Then the payload will be lowered down by the carriages in which the payload is converted from horizontality to verticality. The crane system mainly consists of a twin beam, two carriages, a cylindrical payload, and two wire ropes. It is considered as a dynamic model, which can be employed for the dynamic response analysis of the crane system.

Systems of a beam carrying masses are frequently used as design models in engineering. Generally,

studies [1–10] have focused on natural frequencies and mode shapes of mass-loaded beams associated with different boundary conditions. Cha [3] has generally summarized the researches about the approximate and exact analyses and classified the analysing approaches commonly used (i.e. the Lagrange multipliers formalism, dynamic Green's function approach, Laplace transform with respect to the spatial variable approach, and the analytical–numerical combined method).

Although a wealth of articles concern the vibration analyses of structures with rigidly attached or elastically mounted equipments, fewer investigations have been made in the crane industry. Oguamanam *et al.* [11, 12] have done the researches on dynamics for an overhead crane, which is modelled as a point mass carriage traversing a simply supported Euler–Bernoulli beam and suspending the payload vibrating in and out of plane via a massless beam, in 1998 and 2001. Yang *et al.* [13] have studied the dynamics of a tower crane handling the payload via rotation and moving the carriage simultaneously, in which the

*Corresponding author: Xi'an Research Institution of Hi-Tech, Hong-qing Town, Xi'an, People's Republic of China.
email: xiaoguang_yao@sina.com

crane was modelled as a system consisting of a flexible clamped-free beam with the spherical payload pendulum that moves along the beam. The authors presented that the following two features distinguish the moving mass problem in the crane industry from that in civil engineering. The first is that the structure on which the moving mass moves always has travelling or rotating motion. The second is that the payload of a crane is attached via cables to a carriage moving along the structure. Thus, the dynamics of an overhead or rotary tower crane includes both the vibration of the structure and the dynamics of the payload pendulum. Some studies [14] on the quayside container crane with double carriage can be obtained; however, in such a system, the two carriages transfer the payloads separately. Hence, they are distinct from the system presented in this article.

Unfortunately, the information on such a special system in which two carriages traverse the beam and suspend the payload synchronously is rare. The object of this article is to present a thorough mathematical analysis model for the uprising dynamics of such a double-carriage overhead crane. The uprising phase can be divided into three subphases (i.e. the empty run, and the pre-tensing and lifting phases). This article mainly focuses on the last two subphases, which can be considered as forced and free vibration processes, respectively. The study can be the foundation of dynamic design and stress calculation of the crane system in the uprising phase.

2 DESCRIPTION OF THE SYSTEM

Figure 1 illustrates the trans-shipment process of the special crane system. From the figure, one can see that

the system can hardly be abstracted as a model only consisting of lumped masses and springs, which cannot accurately describe the dynamic characteristics of the investigated system. The two carriages suspend the rigid payload via two wire ropes and vibrate on the twin beam. Thus, the components inevitably affect each other due to the interactional structure of the system. The interaction induces the distinctive dynamic characteristic (i.e. coupling). Accordingly, a new analytical model is required to depict the dynamics of the special crane system. Before modelling, some assumptions are put forward to give prominence to the main characteristics and simplify the minor ones of the physical crane system.

1. The crane system can be divided into two identical subsystems due to the symmetry of the structure and payload about the vertical plane xoy . Therefore, the twin beam can be simplified to a single one and the mass properties of the components should be reduced to half of the physical values.
2. The beam can be considered as a simply supported beam of rectangular cross-section with uniform material properties. The carriage, payload, and wire rope are considered as lumped mass, rigid body, and spring, respectively.
3. System vibrations are assumed only occurring in the xoy plane; thus, the out-of-plane vibrations are ignored.
4. If the length alteration of the wire rope is less than 5 per cent of the whole length, the stretching stiffness of the rope can be regarded as invariable.
5. Damping can always be ignored in the calculation of the maximum dynamic load.

According to the aforementioned assumptions, the dynamic study of the crane system can then be

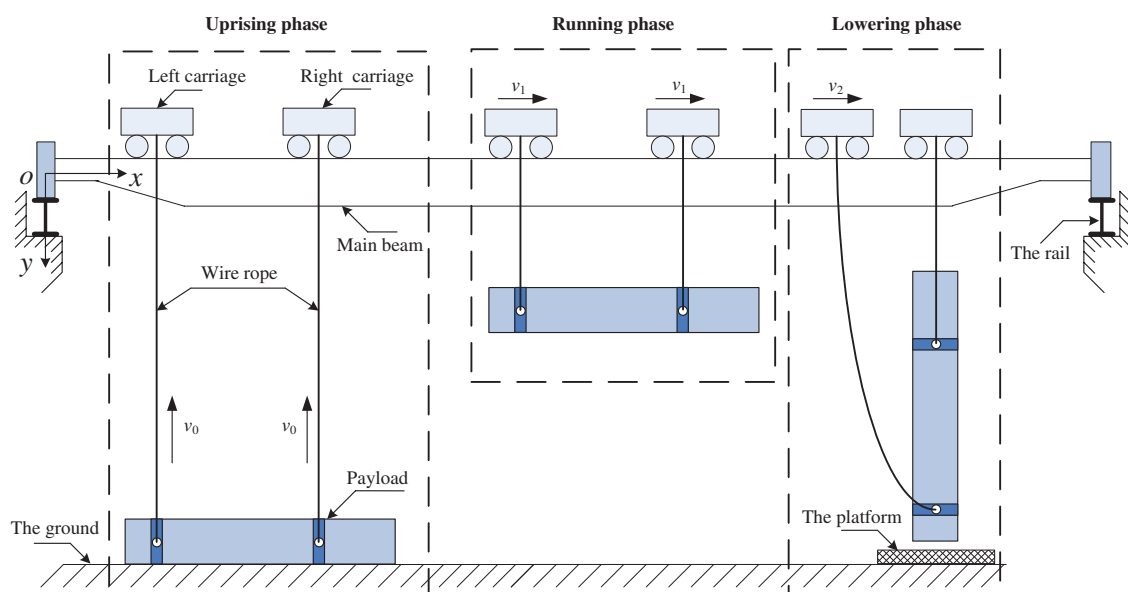


Fig. 1 Diagrammatic sketch of the trans-shipment process of a double-carriage crane system

converted into the study of a mass–beam–payload system.

3 VIBRATION ANALYSIS OF A SIMPLY SUPPORTED BEAM CARRYING LUMPED MASSES

The associated problems of the mass-loaded beam have been studied by numerous authors for many years. In the succedent analysis, flexural free vibrations of a uniform Euler–Bernoulli beam, carrying lumped masses, are presented. The flexural vibration equations of the beam can be expressed as

$$\rho A \frac{\partial^2 y(x, t)}{\partial t^2} + \sum_{i=1}^N m_i \delta(x - x_{mi}) \frac{\partial^2 y(x, t)}{\partial t^2} + EI \frac{\partial^4 y(x, t)}{\partial x^4} = 0 \tag{1}$$

The fourth-order partial differential equation can be solved by the method of separation of variables. Before the solution, it is expedient to introduce the following non-dimensional parameters

$$\xi = \frac{x}{l_b}, \quad \xi_i = \frac{x_{mi}}{l_b}, \quad M_i = \frac{m_i}{\rho A l_b} \tag{2}$$

The parameters are introduced to make the formular format more regular and the numerical calculations more accurate. According to the introduced parameters, the analytical solution of equation (1) can then be assumed as [15, 16]

$$y(x, t) = Y(\xi)q(t) \tag{3}$$

where $Y(\xi)$ is the mode shape function of the mass-loaded beam.

Substituting the assumption into equation (1), one can obtain the ordinary differential equation of $Y(\xi)$ as

$$Y^{(4)}(\xi) - \beta^4 Y(\xi) = \beta^4 \sum_{i=1}^N M_i Y(\xi) \delta(\xi - \xi_i) \tag{4}$$

where

$$\beta^4 = \frac{\rho A l_b^4 \omega^2}{EI} \tag{5}$$

Performing Laplace’s transformation [17] on equation (4), one can obtain

$$L[Y(\xi)] = \frac{s^3 Y(0) + s^2 Y'(0) + s Y''(0) + Y'''(0)}{s^4 - \beta^4} + \beta^4 \sum_{i=1}^N M_i Y(\xi_i) \frac{e^{-s \xi_i}}{s^4 - \beta^4} \tag{6}$$

Performing the inverse Laplace’s transformation on equation (6), one can obtain

$$Y(\xi) = Y(0)S(\beta\xi) + Y'(0)T(\beta\xi) + Y''(0)U(\beta\xi) + Y'''(0)V(\beta\xi) + \beta^4 \sum_{i=1}^N M_i Y(\xi_i) V[\beta(\xi - \xi_i)] u(\xi - \xi_i) \tag{7}$$

Equation (7) is the detailed expression of the mode shape function $Y(\xi)$. Thereinto, $S(kx)$, $T(kx)$, $U(kx)$, and $V(kx)$ are the Krylov functions, which can be described as

$$\begin{cases} S(\beta\xi) = \frac{1}{2}(\text{ch } \beta\xi + \cos \beta\xi), \\ T(\beta\xi) = \frac{1}{2\beta}(\text{sh } \beta\xi + \sin \beta\xi) \\ U(\beta\xi) = \frac{1}{2\beta^2}(\text{ch } \beta\xi - \cos \beta\xi), \\ V(\beta\xi) = \frac{1}{2\beta^3}(\text{sh } \beta\xi - \sin \beta\xi) \end{cases} \tag{8}$$

The functions have some useful characteristics, which can be denoted as

$$\begin{cases} S'(\beta\xi) = \beta^4 V(\beta\xi), & T'(\beta\xi) = S(\beta\xi) \\ U'(\beta\xi) = T(\beta\xi), & V'(\beta\xi) = U(\beta\xi) \end{cases} \tag{9}$$

Utilizing equations (8) and (9), one can arrange equation (7) to a more regular form after some algebraic manipulations as [16]

$$Y(\xi) = Y(0) \left\{ S(\beta\xi) + \sum_{i=1}^N V[\beta(\xi - \xi_i)] \times u(\xi - \xi_i) W_1^{(i)}(\beta) \right\} + Y'(0) \left\{ T(\beta\xi) + \sum_{i=1}^N V[\beta(\xi - \xi_i)] \times u(\xi - \xi_i) W_2^{(i)}(\beta) \right\} + Y''(0) \left\{ U(\beta\xi) + \sum_{i=1}^N V[\beta(\xi - \xi_i)] \times u(\xi - \xi_i) W_3^{(i)}(\beta) \right\} + Y'''(0) \left\{ V(\beta\xi) + \sum_{i=1}^N V[\beta(\xi - \xi_i)] \times u(\xi - \xi_i) W_4^{(i)}(\beta) \right\} \tag{10}$$

where

$$\begin{cases} W_1^{(i)}(\beta) \\ = \beta^4 M_i \left\{ S(\beta \xi_i) + \sum_{j=1}^{i-1} V[\beta(\xi_{j+1} - \xi_j)] W_1^{(j)}(\beta) \right\} \\ W_2^{(i)}(\beta) \\ = \beta^4 M_i \left\{ T(\beta \xi_i) + \sum_{j=1}^{i-1} V[\beta(\xi_{j+1} - \xi_j)] W_2^{(j)}(\beta) \right\} \\ W_3^{(i)}(\beta) \\ = \beta^4 M_i \left\{ U(\beta \xi_i) + \sum_{j=1}^{i-1} V[\beta(\xi_{j+1} - \xi_j)] W_3^{(j)}(\beta) \right\} \\ W_4^{(i)}(\beta) \\ = \beta^4 M_i \left\{ V(\beta \xi_i) + \sum_{j=1}^{i-1} V[\beta(\xi_{j+1} - \xi_j)] W_4^{(j)}(\beta) \right\} \end{cases}$$

are introduced as operation symbols.

The boundary conditions of a simply supported beam can be described as $Y(0) = Y''(0) = 0$ and $Y(1) = Y''(1) = 0$. Substituting the boundary conditions into equation (10) and setting the corresponding determinant of coefficients to zero, one can obtain the following transcendental frequency equation of the mass-loaded beam

$$\begin{vmatrix} T(\beta) + \sum_{i=1}^N V[\beta(1 - \xi_i)] W_2^{(i)}(\beta) \\ V(\beta) + \sum_{i=1}^N V[\beta(1 - \xi_i)] W_4^{(i)}(\beta) \\ \beta^4 V(\beta) + \sum_{i=1}^N T[\beta(1 - \xi_i)] W_2^{(i)}(\beta) \\ T(\beta) + \sum_{i=1}^N T[\beta(1 - \xi_i)] W_4^{(i)}(\beta) \end{vmatrix} = 0 \quad (11)$$

Equation (11) is a transcendental equation about β , which can be used to evaluate the eigenfrequency ω in equation (5) and the eigenmode $Y(\xi)$ according to the boundary conditions.

4 DYNAMIC RESEARCH IN THE PRE-TENSING PHASE

At the end of empty run, it is assumed that the uprising velocity of the drop-hanger has achieved the nominal value v_0 . The payload does not take part in the vibration as it lies on ground all the time in the pre-tensing phase. The crane system in this phase can then be equalled to a dynamic model illustrated in Fig. 2. In the model, the beam is considered as a simply supported uniform Euler–Bernoulli beam and the carriages are considered as two lumped masses attached

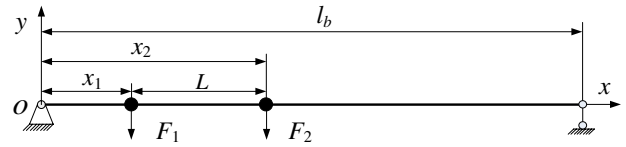


Fig. 2 Dynamic model of pre-tensing phase

to the beam. The mass-loaded beam is motivated by two external forces deriving from the elasticity of the ropes. Kinetic energy of the system consists of the contributions from the beam $T_b(t)$ and the carriages $T_c(t)$. They can be expressed as

$$T_b(t) = \int_0^{l_b} \frac{1}{2} \rho A [\dot{y}(x, t)]^2 dx \quad (12)$$

$$T_c(t) = \frac{1}{2} m_1 \dot{y}^2(x_1, t) + \frac{1}{2} m_2 \dot{y}^2(x_2, t) \quad (13)$$

Potential energy of the system consists of the contribution from the beam $U_b(t)$, which can be expressed as

$$U_b(t) = \frac{1}{2} \int_0^{l_b} EI \left[\frac{\partial^2 y(x, t)}{\partial x^2} \right]^2 dx \quad (14)$$

Using the non-dimensional co-ordinate ξ , the elastic displacement of the beam $y(x, t)$ can be assumed such that

$$y(x, t) = l_b \mathbf{Y}(\xi)^T \mathbf{q}(t) \quad (15)$$

where $\mathbf{q}(t) = [q_1(t) q_2(t) \dots q_n(t)]^T$ is the column vector of undetermined coefficients and $\mathbf{Y}(\xi) = [Y_1(\xi) Y_2(\xi) \dots Y_n(\xi)]^T$ is the column vector of basis functions, which in this case are the orthonormal eigenfunctions of a mass-loaded beam with simply supported boundary conditions. The orthonormal eigenfunctions $\mathbf{Y}(\xi)$ are determined by equation (11) and the boundary conditions. Furthermore, the orthogonality can be deduced as

$$\int_0^1 \mathbf{Y}(\xi) \mathbf{Y}(\xi)^T d\xi + M_1 \mathbf{Y}(\xi_1) \mathbf{Y}(\xi_1)^T + M_2 \mathbf{Y}(\xi_2) \mathbf{Y}(\xi_2)^T = \mathbf{I} \quad (16)$$

$$\int_0^1 \mathbf{Y}''(\xi) \mathbf{Y}''(\xi)^T d\xi = \Lambda_\beta^4 = \text{diag}(\beta_1^4, \beta_2^4, \dots, \beta_n^4) \quad (17)$$

where $\Lambda_\beta = \text{diag}(\beta_1, \beta_2, \dots, \beta_n)$ is a diagonal matrix of $\beta_i (i = 1, 2, \dots, n)$.

The generalized force, $\mathbf{F}_g(t) = [F_{g1}(t) F_{g2}(t), \dots, F_{gn}(t)]^T$, of the system can be derived utilizing the principle of virtual power. The manipulation process can be described in particular as

$$\begin{aligned} \delta W(t) &= F_1(t) \delta y(x_1, t) + F_2(t) \delta y(x_2, t) \\ &= \delta \mathbf{q}^T(t) [F_1(t) l_b \mathbf{Y}(\xi_1) + F_2(t) l_b \mathbf{Y}(\xi_2)] \end{aligned} \quad (18)$$

Thus, the generalized force can be expressed as

$$\mathbf{F}_g(t) = F_1(t)l_b\mathbf{Y}(\xi_1) + F_2(t)l_b\mathbf{Y}(\xi_2) \quad (19)$$

where $F_1(t) = -k_1v_0t$ and $F_2(t) = -k_2v_0t$ are the external forces motivating at the co-ordinates x_1 and x_2 .

Some dimensional ratios and a non-dimensional parameter are also introduced such that

$$\begin{aligned} K_1 &= \frac{k_1}{\rho Al_b}, & K_2 &= \frac{k_2}{\rho Al_b}, & V_0 &= \frac{v_0}{l_b}, \\ \Omega^2 &= \frac{g}{l_b} & \text{and} & & M &= \frac{m}{\rho Al_b} \end{aligned} \quad (20)$$

Ignoring dissipation energy according to assumption (5), one can obtain the dynamic equation of the system in the pre-tensing phase substituting equations (12) to (14) and (19) into Lagrange's equation as

$$\ddot{\mathbf{q}}(t) + \mathbf{\Lambda}_\omega^2 \mathbf{q}(t) + [K_1 V_0 \mathbf{Y}(\xi_1) + K_2 V_0 \mathbf{Y}(\xi_2)]t = \mathbf{0} \quad (21)$$

where $\mathbf{\Lambda}_\omega = \text{diag}(\omega_1, \omega_2, \dots, \omega_n)$ is a diagonal matrix of the eigenfrequencies $\omega_i (i = 1, 2, \dots, n)$. Equation (21) can be solved by the numerical method, setting the initial conditions to zero in the pre-tensing phase.

The finish time t_1 of the pre-tensing phase can be defined as the time when the summation of the external elastic forces achieves the gravity of the payload. Then the payload will leave the ground and the balance equation of external forces and gravity can be expressed as

$$K_1[V_0 t + \mathbf{Y}(\xi_1)^T \mathbf{q}(t)] + K_2[V_0 t + \mathbf{Y}(\xi_2)^T \mathbf{q}(t)] = M\Omega^2 \quad (22)$$

The finish time t_1 is determined by equation (22) and the vibration states of the system at that time are the initial values for the lifting phase.

5 DYNAMIC RESEARCH IN LIFTING PHASE

In the lifting phase, all components participate in the vibration. The crane system can be equalled to a dynamic model illustrated in Fig. 3. The main beam and carriages are considered as Euler–Bernoulli beam and lumped masses as in Fig. 2. The wire ropes are considered as springs and the payload is considered as a rigid cylinder.

Kinetic energy in this phase is composed of contributions from the beam $T_b(t)$, carriages $T_c(t)$, and the payload $T_p(t)$. Descriptions of the kinetic energy $T_b(t)$ and $T_c(t)$ are identical to equations (12) and (13). The displacement of the payload mass centre $y(t)$ is

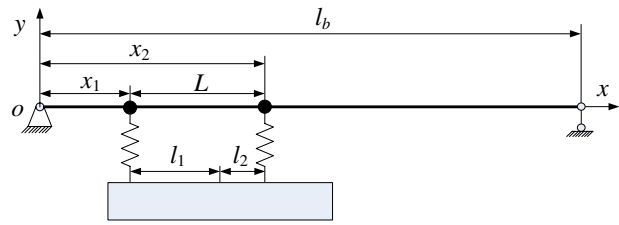


Fig. 3 Dynamic model of lifting phase

defined as

$$y(t) = y_c(t) - y_{c0} \quad (23)$$

Therefore, one can describe kinetic energy of the payload $T_p(t)$ as

$$T_p(t) = \frac{1}{2} m \dot{y}^2(t) + \frac{1}{2} J_c \dot{\theta}_c^2(t) \quad (24)$$

Potential energy in this phase is composed of contributions from the beam $U_b(t)$ and wire ropes $U_w(t)$. Similarly, $U_b(t)$ is identical to equation (14) and one can describe the potential energy of the wire ropes $U_w(t)$ as

$$\begin{aligned} U_w(t) &= \frac{1}{2} k_1 \{y(x_1, t) - [y(t) + \theta_c(t)l_1 - v_0 t]\}^2 \\ &+ \frac{1}{2} k_2 \{y(x_2, t) - [y(t) - \theta_c(t)l_2 - v_0 t]\}^2 \end{aligned} \quad (25)$$

Before the formular arrangement, it is expedient to introduce the following symbol vectors and matrices

$$\begin{aligned} \alpha_1^T &= [1, -l_1], & \alpha_2^T &= [1, l_2], & \alpha_3^T &= [1, 0], \\ \mathbf{Y}_D^T(t) &= \begin{bmatrix} y(t) \\ \theta_c(t) \end{bmatrix}, & \mathbf{M}_D &= \text{diag} \left(\frac{m}{\rho Al_b}, \frac{J_c}{\rho Al_b} \right) \end{aligned} \quad (26)$$

The generalized independent variable in energy functions are specified as $[\mathbf{q}^T(t) \mathbf{Y}_D^T(t)]^T$ and, furthermore, the differential equations in the lifting phase are derived substituting equations (12) to (14), (24), and (25) into the Lagrange's equation as

$$\begin{aligned} \ddot{\mathbf{q}}(t) &+ [\mathbf{\Lambda}_\omega^2 + K_1 \mathbf{Y}(\xi_1) \mathbf{Y}(\xi_1)^T + K_2 \mathbf{Y}(\xi_2) \mathbf{Y}(\xi_2)^T] \mathbf{q}(t) \\ &- [K_1 \mathbf{Y}(\xi_1) \alpha_1^T + K_2 \mathbf{Y}(\xi_2) \alpha_2^T] \mathbf{Y}_D(t) \\ &+ [K_1 \mathbf{Y}(\xi_1) + K_2 \mathbf{Y}(\xi_2)] V_0 t = \mathbf{0} \end{aligned} \quad (27)$$

$$\begin{aligned} \mathbf{M}_D \ddot{\mathbf{Y}}_D(t) &+ (K_1 \alpha_1 \alpha_1^T + K_2 \alpha_2 \alpha_2^T) \mathbf{Y}_D(t) \\ &- [K_1 \mathbf{Y}(\xi_1) \alpha_1^T + K_2 \mathbf{Y}(\xi_2) \alpha_2^T] \mathbf{q}(t) \\ &- (K_1 \alpha_1 + K_2 \alpha_2) V_0 t = \mathbf{0} \end{aligned} \quad (28)$$

Equations (27) and (28) can be solved simultaneously by the numerical method with the initial conditions determined by equations (21) and (22).

6 NUMERICAL EXAMPLES

This section is devoted to the numerical evaluations of the dynamic equations obtained in the aforementioned studies. It is known that the work condition in the early stage of a crane system can always be one of the worst conditions. Therefore, this section mainly focuses on the dynamic responses in the pre-tensing and initial lifting phases. Parameter values of structure and mass properties of the crane system are listed in Table 1. The cross-section configuration of the main beam is illustrated in Fig. 4 and the sectional dimensions are listed in Table 2. Cross-sectional inertia moment of the beam can be calculated as $I = 9.0 \times 10^{-3} \text{ m}^4$ according to the formula

$$I = \frac{[(h_1 + h_2)h^3 + (h_3^3 + h_4^3)b]}{12} + b(h_3 + h_4) \left(\frac{h}{2}\right)^2 \tag{29}$$

According to assumption (4), the duration employed in dynamic calculation is set to 3 s. Length alternation in the duration can be calculated as

$$\Delta l = \frac{v_0 t}{l_0} = \frac{0.133 \times 3}{14.25} = 2.8 \text{ per cent} \tag{30}$$

Table 1 Parameter values of the crane system

m	10^4 kg	J_c	$3 \times 10^4 \text{ kg m}^2$	m_b	10^4 kg
h_b	19.5 m	l_0	14.25 m	y_{c0}	-14.25 m
v_0	0.133 m/s	D	0.018 m	L	3.7 m
a_1	2 m	l_1	2.3 m	m_1	$2.0 \times 10^3 \text{ kg}$
a_2	5.7 m	L_2	1.4 m	m_2	$2.0 \times 10^3 \text{ kg}$

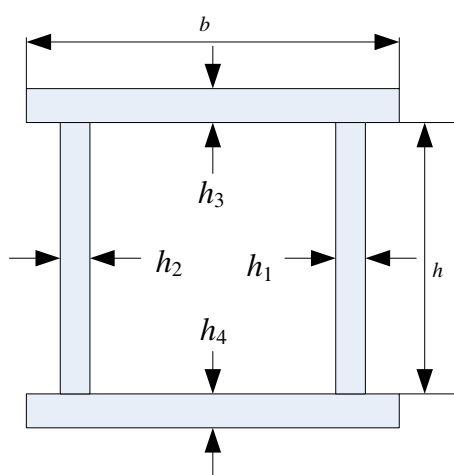


Fig. 4 Cross-section of the main beam

Table 2 Sectional dimensions of the main beam

h_1	0.006 m	h_2	0.006 m	h	1.55 m
h_3	0.008 m	h_4	0.008 m	b	0.55 m

Table 3 Parameter values in calculation of wire rope stiffness

E	D	α_1	α_2	l_k
$2.06 \times 10^{11} \text{ N/m}^2$	0.018 m	$13 \sim 16^\circ$	$16 \sim 18^\circ$	14.25 m

which is smaller than 5 per cent. Thus, the stiffness of wire rope can be considered invariable and calculated as $k = 2.5 \times 10^6 \text{ N/m}$ by the formula

$$k = \frac{\pi D^2 E \cos^4 \alpha_1 \cos^4 \alpha_2}{4l_k} \tag{31}$$

Parameter values in equation (31) are listed in Table 3.

6.1 Dynamic calculation of the model

The first three eigenfrequencies and eigenmodes, which are calculated by equations (5) and (11) and listed in Table 4, of the mass-loaded beam are employed in calculation. Differential equations are calculated by the fourth Runge–Kutta method in MATLAB. The time step is set as $\Delta t = 0.0005 \text{ s}$ to capture the dynamic response of the system in detail.

Before the interpretation of the calculation results, some supplementary specifications need to be represented that the lifting phase is set temporally independent of the pre-tensing phase, which means that the initial time of lifting phase is set as $t = 0$ but not t_1 , in the numerical calculation.




Displacements and velocities, employed as initial values in the lifting phase, of carriages at the finish time t_1 are listed in Table 5. The finish time t_1 is calculated as 0.304 s.

Figure 5 illustrates the uplifting displacement $y(t)$ of payload mass centre in the lifting phase. From the picture, one can see that the curve increases with a near-linear trend due to the stationary uplifting velocity v_0 of the hanger. Some mild and tiny fluctuations, deriving from the flexibility of wire ropes and beam, can be seen on the curve.

Figure 6 describes the uplifting velocity of the payload mass centre. Conspicuous fluctuations with wave crest value as 0.26 m/s and wave hollow value as 0 m/s can be seen on the graph. The curve has a mean value of 0.13 m/s, which is the uplifting velocity of the hanger. However, the velocity curve does not converge to 0.13 m/s as time goes on and oscillates with the sustained amplitude. The reason for this phenomenon can be derived from the ignoring of system damping in assumption (5).

Figure 7 illustrates the angular displacement of the payload rotating around its mass centre in a lifting motion. The angle curve oscillates between -0.15° and 0.35° and has a mean value of 0.12° , which reflects a fact that the payload is oblique with a clockwise slope and vibrates around the obliquity in the lifting motion

Table 4 Comparison of eigenfrequencies and eigenmodes of mass-loaded beam

Modal order in ADAMS	1st	2nd	3rd
Eigenfrequencies in MATLAB (Hz)	10.6271	40.7298	85.6621
Eigenfrequencies in ADAMS (Hz)	10.5138	39.5935	82.1520
Corresponding eigenmodes			
Relative errors of frequencies (%)	1.07	2.79	4.10

Relative error is defined as $100 \times |MATLAB - ADAMS|/MATLAB$.

Table 5 Initial values of lifting phase (i.e. the final states of pre-tensing phase, and the finish time t_1)

Initial displacement (m)	y_{10} -1.391×10^{-3}	y_{20} -3.272×10^{-3}	Finish time of pre-tensing phase t_1
Initial velocity (m/s)	v_{10} -4.427×10^{-3}	v_{20} -1.050×10^{-2}	0.304 s

y_{10} and y_{20} represent the displacements of carriages at the very beginning of lifting phase. v_{10} and v_{20} represent the corresponding velocities of carriages at that time.

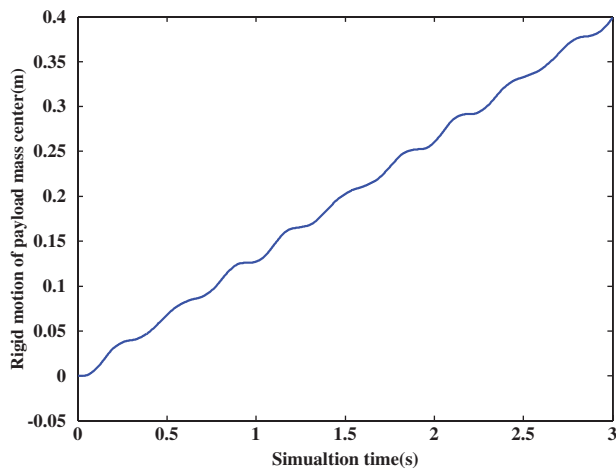


Fig. 5 Displacement of the payload mass centre in lifting motion

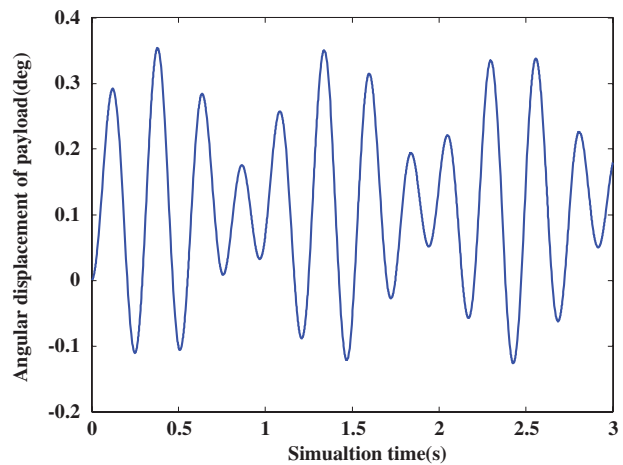


Fig. 7 Angular displacement of payload rotating around its mass centre in lifting motion

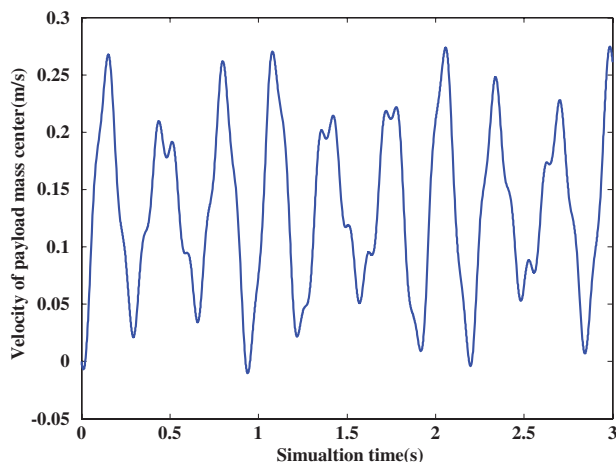


Fig. 6 Velocity of payload mass centre in lifting motion

due to the asymmetry of the two external forces acting on it.

6.2 Calculation of the dynamic load coefficients

It can be evaluated that the maximum vibration amplitude, y_{dmax} , of the beam occurs at the location $x = 9.316$ m. Therefore, the dynamic load coefficient of the beam, φ_1 , at that location can be denoted as

$$\varphi_1 = \frac{y_{dmax}}{y_s} \tag{32}$$

where y_s is the deformation of beam deriving from the static load equivalent to the maximum dynamic load.

The dynamic load coefficient of the payload, φ_2 , is defined as

$$\varphi_2 = \frac{|F_1(t) + F_2(t)|_{max}}{mg} \tag{33}$$

where $|F_1(t) + F_2(t)|_{\max}$ denotes the maximum summation of the external elastic forces, $F_1(t)$ and $F_2(t)$, acting on the payload.

The maximum vibration amplitude y_{dmax} and external forces $F_1(t)$ and $F_2(t)$ can be obtained in numerical calculation. Thus, the dynamic load coefficients φ_1 and φ_2 are evaluated as $\varphi_1 = 1.51$ and $\varphi_2 = 1.29$ according to equations (32) and (33).

7 VALIDITY CHECKING

The models and equations in the pre-tensing and lifting phases can be verified utilizing the dynamic simulation software ADAMS. ADAMS is chosen for the verification; it not only is a well-known engineering software extensively accepted and used by mechanical engineers but also supplies a different approach to evaluate the dynamic response of the crane system.

7.1 Modelling in ADAMS

Modelling process of the main beam can be described as follows. First, the model of the main beam is created in ANSYS; second, the model is divided into 40 cells by beam3 element, which is a uniaxial element with tension, compression, and bending capabilities; third, four interface nodes, interacting with outside, marked as 1–4 are added to the beam; moreover, the rigid sections surrounding the nodes are also defined; and finally, the finite-element model is transformed into a modal neutral file (.mnf), which can be exported into ADAMS to generate the flexible main beam.

Modelling process of the wire rope [18] can be described as follows. The wire rope is dispersed and represented by a large number of short cylinders connected with bushings, as illustrated in Fig. 8. If the cylinders are short enough compared with the whole length of the wire rope, the discrete model can then be considered continuous and represent the stretching and bending characteristics of the wire rope well and truly. The employed cylinder length is set to 20 cm, which is merely 1.5 per cent of the whole length.

The carriages and payload are, respectively, modelled as two cubes and a cylinder with the same mass and dimension properties as the physical objects.

Defining of constraints and motions can be described in particular as follows. Owing to the boundary condition of the main beam, two revolve joints are employed on both ends of the flexible beam at nodes 1 and 4. Two dumbered masses, which are modelled

as the interaction medium, transferring the interaction forces and motions, of the carriages and beam, are fixed at nodes 2 and 3. The carriages and payload are connected by wire ropes via revolve joints. The involution motion of the reel is substituted by translational motion, which is much easier to carry out, of carriage to uplift the payload. Therefore, two translational joints along axis y between the carriages and dumbered masses are added to proffer the translational motions. To balance the gravity of the payload at the pre-tensing phase, a contact force is added between the payload and the ground. The sketch diagram of the dynamic model of the crane system created in ADAMS is illustrated in Fig. 9. The black points, marked as 1–4 from the left to the right end of beam, respectively, represent the four interface nodes.

Defining the translational velocity of carriages as $v_0 = 0.133$ m/s, setting the simulation time as $t = 3$ s, one can carry out the dynamic simulation of the crane system in ADAMS. Corresponding results obtained can be employed for the verifications of those obtained in aforementioned studies.

7.2 Comparison of eigenfrequencies and results

Creating a new model including the flexible beam and two carriages, connecting both ends of the beam to the ground by revolve joints at interface nodes 1 and 4, fixing the two carriages at interface nodes 2 and 3, and removing system gravity, one can obtain eigenfrequencies and eigenmodes of the mass-loaded beam in ADAMS. Comparison of the eigenfrequencies and eigenmodes is listed in Table 4. It can be seen that the eigenmodes are correspondingly identical and the differences between the eigenfrequencies are tiny. The errors are less than 5 per cent, which can be regarded as acceptable from the engineering point of view.

Comparison of some other results is listed in Table 6, which exhibits that errors between the two models are all acceptable. The displacements D_1 , D_2 , D_3 , and dynamic load coefficient φ_1 calculated in MATLAB are smaller than those in ADAMS; however, the maximum summation of wire rope forces and the dynamic load coefficient φ_2 are bigger in MATLAB. Differences are derived from the errors between eigenfrequencies and eigenmodes calculated in the two models. In Table 4, the eigenfrequencies in MATLAB are bigger than those in ADAMS, which implies a higher stiffness of the beam. Therefore, the beam deformation and dynamic load coefficient φ_2 are smaller for the stiffer beam in

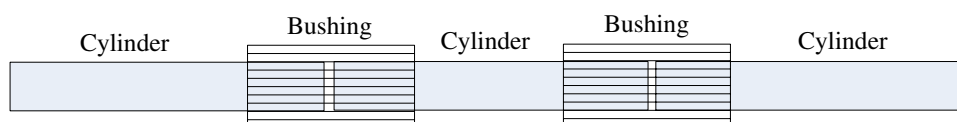


Fig. 8 A section of the wire rope model employed in ADAMS

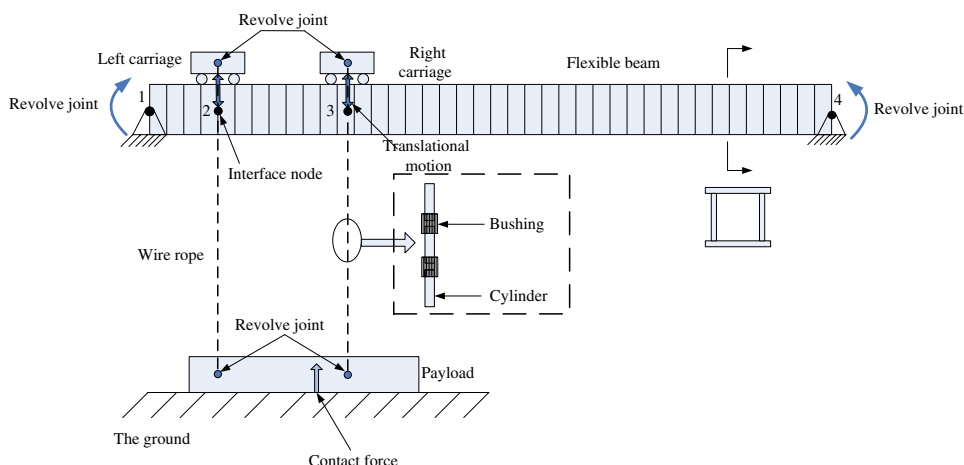


Fig. 9 Dynamic model of the crane system created in ADAMS

Table 6 Comparison of some results

Results	Displacement D_1 (m)	Displacement D_2 (m)	Displacement D_3 (m)	Force F (kN)	Coefficient φ_1	Coefficient φ_2
Value in ADAMS	3.35×10^{-3}	8.37×10^{-3}	9.86×10^{-3}	119.77	1.56	1.22
Value in MATLAB	3.21×10^{-3}	8.19×10^{-3}	9.54×10^{-3}	126.46	1.51	1.29
Relative errors (%)	4.36	2.20	3.35	5.59	3.31	5.43

D_1 denotes the maximum displacement of the left carriage. D_2 denotes the maximum displacement of the right carriage. D_3 denotes the maximum deformation of the beam. F denotes the maximum summation force of the wire ropes. Relative error is defined as $100 \times |\text{MATLAB} - \text{ADAMS}| / \text{MATLAB}$.

MATLAB. On the contrary, the dynamic forces and dynamic load coefficient φ_2 are bigger.

From the comparisons above, one can conclude that the results obtained by the analytical and FE models show good agreements. Errors between the two models are tiny and can be considered acceptable. The latter model can be the validity evidence for the former one. Therefore, the models and equations, obtained in the aforementioned studies, can be considered feasible and reliable.

8 CONCLUSIONS

In this article, the dynamics of an overhead crane, carrying two carriages and payload, in pre-tensing and lifting phases has been studied. The analytical model of the crane system, consisting of the beam, lump masses, rigid body, and springs, differs from the prior models that include only point masses and springs. The most distinguished characteristic is the dynamic coupling deriving from the distributed mass beam, lump masses, and rigid body. Differential equations in the pre-tensing and lifting phases are derived substituting the kinetic and potential energy functions of the system into Lagrange's equation. The equations are solved by a numerical method with the corresponding initial values.

The identical crane system is studied by a different approach, in which a rigid and flexible coupling model

of the system is created by ANSYS and ADAMS. Comparisons of the results are listed and analysed. It can be observed that errors between the two approaches are acceptable and the results show good agreements. Thus, the analytical models and differential equations can be considered feasible and reliable. Furthermore, it can proffer valuable references for modelling and analysing other similar engineering problems.

ACKNOWLEDGEMENT

The author wishes to express his sincere thanks to the reviewer for useful and important comments.

© Authors 2011

REFERENCES

- 1 **Low, K. H.** An analytical-experimental comparative study of vibration analysis for loaded beams with variable boundary conditions. *Comput. Struct.*, 1997, **65**(1), 97–107.
- 2 **Low, K. H.** A comparative study of the eigenvalue solutions for mass-loaded beams under classical boundary conditions. *Int. J. Mech. Sci.*, 2001, **43**, 237–244.
- 3 **Cha, P. D. and Wong, W. C.** A novel approach to determine the frequency equation of combined dynamical systems. *J. Sound Vibr.*, 1999, **219**, 689–706.

- 4 **Cha, P. D.** Eigenvalues of a linear elastic carrying lumped masses, springs and viscous dampers. *J. Sound Vibr.*, 2002, **257**, 798–808.
- 5 **Cha, P. D.** A general approach to formulating the frequency equation for a beam carrying miscellaneous attachments. *J. Sound Vibr.*, 2005, **286**, 921–939.
- 6 **Alsaif, K.** and **Foda, M. A.** Vibration suppression of a beam structure by intermediate masses and springs. *J. Sound Vibr.*, 2002, **256**(4), 629–645.
- 7 **Yadav, D., Kamle, S.,** and **Talukdar, S.** Transverse vibration of multi mass loaded variable section beams under random excitation. *J. Sound Vibr.*, 1997, **207**, 151–173.
- 8 **Keltie, R. E.** and **Cheng, C. C.** Vibration reduction of a mass-loaded beam. *J. Sound Vibr.*, 1995, **187**(2), 213–228.
- 9 **Gürgöze, M.** On the alternative formulations of the frequency equation of a Bernoulli–Euler beam to which several spring–mass systems are attached in-span. *J. Sound Vibr.*, 1998, **217**, 585–595.
- 10 **Wu, J. S.** and **Chou, H. M.** A new approach for determining the natural frequencies and mode shapes of a uniform beam carrying any number of spring masses. *J. Sound Vibr.*, 1999, **220**, 451–468.
- 11 **Oguamanan, D. C. D., Hansen, J. S.,** and **Heppler, G. R.** Dynamic response of an overhead crane system. *J. Sound Vibr.*, 1998, **213**(5), 889–906.
- 12 **Oguamanan, D. C. D., Hansen, J. S.,** and **Heppler, G. R.** Dynamics of a three-dimensional overhead crane system. *J. Sound Vibr.*, 2001, **242**(3), 411–426.
- 13 **Yang, W. Q., Zhang, Z. Y.,** and **Shen, R. Y.** Modeling of system dynamics of a slewing flexible beam with moving payload pendulum. *Mech. Res. Commun.*, 2007, **34**, 260–266.
- 14 **Tong, M. H.** *Structural dynamic response of double carriage container crane* (in Chinese). Master Dissertation, Shanghai Maritime University, 2004.
- 15 **Xia, J., Zhu, M. C.,** and **Ma, D.Y.** Analysis of lateral natural vibration of beams with lumped masses and elastic supports (in Chinese). *J. Southwest Inst. Technol.*, 1999, **14**(4), 1–4.
- 16 **Peng, X.** and **Peng, F.** New analytical expressions of lateral vibration characteristics of a beam with lumped masses (in Chinese). *J. Hunan Univ. Nat. Sci. Ed.*, 2002, **29**(1), 43–48.
- 17 Mathematical Teaching and Research Group of Nanjing Engineering College. *Integral Transformation*, 1982 (Higher Education Publishing Company, Beijing, China).
- 18 **Wang, D. S., Kong, D. W.,** and **Zhao, K. L.** Modeling methods for wire cables of mining excavator by MSC ADAMS (in Chinese). *Comput. Aided Eng.*, 2006, **15**, 364–366.

APPENDIX

Notation

a	cross-sectional area of the main beam
ADAMS	automatic dynamic analysis of mechanical system
d	virtual value of wire rope diameter
E	elastic modulus

$F_g(t)$	generalized force of system
$F_1(t), F_2(t)$	elastic external forces of the wire ropes
I	inertia moment of the beam cross-section
J_c	rotary inertia of the payload with respect to its mass centre
k_1, k_2	stiffness of the wire ropes
l_1, l_2	distances of the payload mass centre as measured from the left and right suspension points of wire rope
l_b	span of the beam
l_k	virtual value of the wire rope length
l_0	initial length of the wire rope
L	distance of the carriage mass centres
m	mass of the uplifting payload
m_1, m_2	mass of the left and right carriage
m_b	mass of the beam
m_i	mass of the i th lumped mass on the beam
n	order of truncation modal basis
N	total number of lumped masses
o	origin of co-ordinate
$q(t)$	modal co-ordinate vector
t	time
t_1	finish time of pre-tensing phase
$T_b(t), T_c(t), T_p(t)$	kinetic energies of the beam, carriage, and payload
$u(x)$	Unit step function
$U_b(t), U_w(t)$	potential energies of the beam and wire rope
v_0	nominal uprising velocity
x	axial co-ordinate (horizontal)
x_{mi}	co-ordinate of the i th lumped mass on the beam
y	transverse co-ordinate (vertical)
$y(t)$	displacement of payload
$y(x, t)$	transverse displacement of the beam at co-ordinate x and time t
y_{c0}	initial co-ordinate of payload mass centre along axis y
$y_c(t)$	co-ordinate of payload mass centre at time t along axis y
y_{dmax}	maximum dynamic vibration amplitude of the main beam
y_s	static deformation amplitude of the main beam
$Y(\xi)$	eigenmode vector of the mass-loaded beam
α_1	spiral angle of the wire rope

α_2	skew angle of strand and rope axis	ω	circular frequency of the beam
β	non-dimensional circular frequency of beam	<i>Superscripts</i>	
δ	Dirac function		
$\theta_c(t)$	rotation angle around the mass centre	'	derivative with respect to spatial variable x
ξ	non-dimensional axial co-ordinate	·	derivative with respect to temporal variable t
ρ	density of the main beam	<i>Subscript</i>	
φ_1, φ_2	dynamic load coefficients of beam and payload	c	mass centre